

PAPER • OPEN ACCESS

PVAL breast phantom for dual energy calcification detection

To cite this article: V Koukou *et al* 2015 *J. Phys.: Conf. Ser.* **637** 012013

View the [article online](#) for updates and enhancements.

You may also like

- [The creation of breast lesion models for mammographic virtual clinical trials: a topical review](#)
Astrid Van Camp, Katrien Houbrechts, Lesley Cockmartin et al.
- [Visualizing microcalcifications in lumpectomy specimens: an exploration into the clinical potential of carbon nanotube-enabled stationary digital breast tomosynthesis](#)
Connor Puett, Jenny Gao, Andrew Tucker et al.
- [The effect of system geometry and dose on the threshold detectable calcification diameter in 2D-mammography and digital breast tomosynthesis](#)
Andria Hadjipanteli, Premkumar Elangovan, Alistair Mackenzie et al.



ECS
The
Electrochemical
Society
Advancing solid state &
electrochemical science & technology

DISCOVER
how sustainability
intersects with
electrochemistry & solid
state science research

PVAL breast phantom for dual energy calcification detection

V. Koukou¹, N. Martini¹, K. Velissarakos², D. Gkremos², C. Fountzoula³, A. Bakas⁴, C. Michail², I. Kandarakis² and G. Fountos²

¹ Department of Medical Physics, Medical School, University of Patras, Rion, Patras, Greece

² Radiation Physics, Materials Technology and Biomedical Imaging Laboratory, Department of Biomedical Engineering, Technological Educational Institute of Athens, Egaleo, Athens, Greece

³ Department of Medical Laboratories, Technological Educational Institute of Athens, Egaleo, Athens, Greece

⁴ Medical Radiological Technology, Faculty of Health and Caring Professions, Technological Educational Institute of Athens, Egaleo, Athens, Greece

E-mail: gfoun@teiath.gr

Abstract. Microcalcifications are the main indicator for breast cancer. Dual energy imaging can enhance the detectability of calcifications by suppressing the tissue background. Two digital images are obtained using two different spectra, for the low- and high-energy respectively, and a weighted subtracted image is produced. In this study, a dual energy method for the detection of the minimum breast microcalcification thickness was developed. The used integrated prototype system consisted of a modified tungsten anode X-ray tube combined with a high resolution CMOS sensor. The breast equivalent phantom used was an elastically compressible gel of polyvinyl alcohol (PVAL). Hydroxyapatite was used to simulate microcalcifications with thicknesses ranging from 50 to 500 μm . The custom made phantom was irradiated with 40kVp and 70kVp. Tungsten (W) anode spectra filtered with 100 μm Cadmium and 1000 μm Copper, for the low- and high-energy, respectively. Microcalcifications with thicknesses 300 μm or higher can be detected with mean glandular dose (MGD) of 1.62mGy.

1. Introduction

Breast cancer is a major public health concern [1]. Microcalcifications are the principal indicator of breast cancer [2], thus the visualization and detection of microcalcifications is significant [2,3]. Dual energy (DE) imaging can enhance the detectability of calcifications by suppressing the tissue background structures [3]. With this technique, separate low- and high-energy images are acquired and a weighted subtracted image is produced.

Previous research works in dual energy imaging showed that the minimum detectable calcification size ranges from 300-355 μm depending on the X-ray technique and the detection system [4,5]. Various tissue-equivalent-phantoms have been used for the experimental validation of these methods [4,5].



In this study, a dual energy imaging method is proposed for the early microcalcification detection. The prototype system used consisted of a modified tungsten (W) anode X-ray tube combined with a high resolution complementary-metal-oxide-semiconductor (CMOS) sensor. The breast equivalent phantom used was an elastically compressible gel of polyvinyl alcohol (PVAL). Contrast to noise ratio in the subtracted (dual energy) image (CNR_{DE}) was calculated for all the examined calcifications, while preserving MGD mean glandular dose (MGD) within examination levels [6].

2. Materials and Methods

Weighted log-subtraction was used to generate the DE subtraction images, $\ln(DE) = \ln(HE) - w\ln(LE)$ where HE and LE are the high- and the low-energy images, and w is the weighting factor [7].

Experiments were carried out in a modified radiographic unit. A Del Medical Eureka X-ray tungsten (W) radiography tube was used with total inherent filtration of 3mm of aluminum (Al) [8]. The low-energy images were acquired at 40kVp with a cadmium (Cd) filter of 100 μ m thickness placed at the tube exit. For the high-energy images, a copper (Cu) filter of 1000 μ m thickness was placed in the beam at 70kVp. The detection system consisted of a terbium-activated gadolinium oxisulfide ($Gd_2O_2S:Tb$) phosphor screen (Min-R 2190 with a mass thickness of 33.91mg/cm²) coupled to a CMOS photodiode pixel array (Remote RadEye HR) [9,10]. The CMOS photodiode array has a format of 1200x1600 pixels with a pitch of 22.5 μ m. The source to image receptor distance (SID) was set at 66cm. A large (1.2mm nominal) X-ray tube focal spot was selected.

The breast phantom used in the experiments of this study was an elastically compressible gel of polyvinyl alcohol (PVAL). A similar breast phantom of PVAL in ethanol and water was developed by Price *et al.* A solid yet elastically compressible gel was produced after being frozen and defrosted [11]. The linear attenuation coefficient of PVAL gels, with different concentrations ranging from 5% to 20% w/v (weight to volume), was in the range of 0.76 to 0.86cm⁻¹ at 17.5keV. These values are very similar to the published breast tissue data at this energy, 0.8-0.9cm⁻¹. The breast tissue equivalent phantom used in this study was produced by mixing 50% ethanol, 50% water and 10% PVAL. The phantom thickness was 4cm. Figure 1 shows the mass attenuation coefficient of PVAL and breast tissue (ICRU-44) using published data [12]. As it can be seen from the plot, the coefficients are identical. The densities of the PVAL and breast tissue are 0.924g/cm³ and 1.020g/cm³ respectively, while the corresponding effective atomic numbers Z are 7.05 and 7.07 [13]. Three PMMA slabs of different thicknesses (0.2, 0.3 and 0.4cm) were used, in order to construct the phantom of microcalcifications (μC). In each PMMA slab, holes were opened and filled with a mixture of hydroxyapatite and epoxy resin (density 1g/cm³) in order the amount of the HAp in each hole to correspond at a specific microcalcification thickness. The thicknesses of the calcifications in the μC phantoms ranged from: (i) 50 to 250 μ m in the 0.2cm thick μC phantom, (ii) 150 to 375 μ m in the 0.3cm thick μC phantom, and (iii) 100 to 500 μ m in the 0.4cm thick μC phantom.

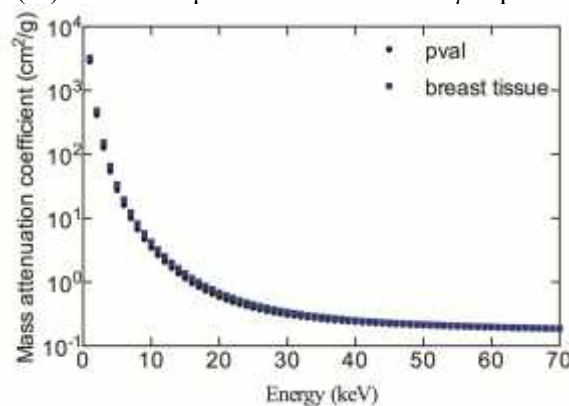


Figure 1. Mass attenuation coefficients of PVAL and breast tissue (ICRU-44).

CNR was used as a measure of image quality and is a function of both the low- and high-energy images. The CNR_{DE} was calculated according to the following equation [14]:

$$CNR_{DE} = \frac{|S_C - S_B|}{\sigma_B} \quad (1)$$

where μ_C and B denote the mean signal of the microcalcification and background regions, and σ represents the standard deviation of pixel values in the background [14]. The CNR_{DE} threshold value for the detection of a calcification was equal to 3 [3].

The MGD was calculated using the practical relation of ACR [15] and previously published data [16].

3. Results and Discussion

Figure 2 shows the dual energy images of homogenous PVAL phantom combined with the examined three-calcification phantoms. The entrance dose was 1.92mGy, corresponding to MGD value of 1.62mGy.

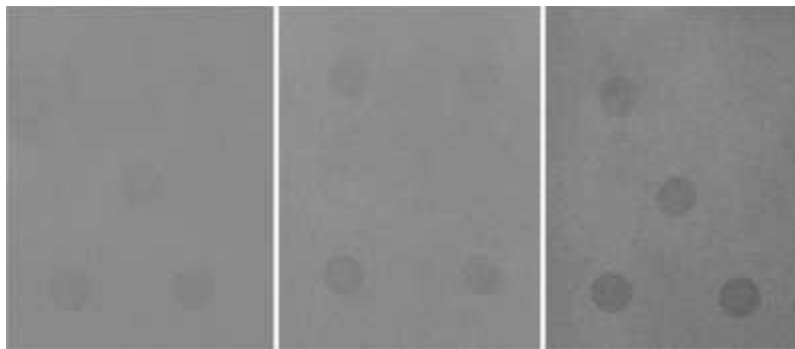


Figure 2. Dual energy images of the three-calcification phantoms of 0.2cm (left), 0.3cm (center) and 0.4cm (right) thick.

Table 1 shows the measured CNR_{DE} values of the three-calcification phantoms, with thicknesses ranging from 150 to 500 μ m for MGD values of 1.62 and 0.80mGy. Calcification thicknesses of 50 and 100 μ m could not be depicted in the DE image due to: (i) counting statistics leading to increase of image noise and (ii) low object contrast which was expected from the simulation study [17]. For this reason, CNR_{DE} values were not included in Table 1. The minimum detectable calcification thickness was 300 μ m, as yielded a CNR_{DE} value of 3.25 which is above the threshold of 3. In a previous dual energy study, the minimum detectable calcification size was reduced to 250 μ m after applying noise reduction techniques in the DE images [5]. However, in this study, noise reduction methods were not included.

Table 1. Measured CNR_{DE} values of the three-calcification phantoms.

Calcification thickness (μ m)	CNR_{DE} (MGD=1.62mGy)	CNR_{DE} (MGD=0.80mGy)
150	1.71	0.79
200	2.11	1.39
225	2.53	1.41

250	2.58	1.97
300	3.25	2.31
375	3.38	2.56
400	3.71	2.65
500	4.63	3.01

4. Conclusions

In this study, a homogenous breast-equivalent-phantom was developed using polyvinyl alcohol, water and ethanol. A mixture of hydroxyapatite and epoxy resin was used for microcalcifications with various thicknesses. Contrast to noise ratio was calculated from the DE subtracted images. The minimum detectable calcification thickness was 300 μ m for mean glandular dose of 1.62mGy.

Acknowledgement

This research has been co-funded by the European Union (European Social Fund) and Greek national resources under the framework of the “Archimedes III: Funding of Research Groups in TEI of Athens” project of the “Education & Lifelong Learning” Operational Programme.

References

- [1] World Health Organization 2009 Available via: http://www.who.int/gender/women_health_report/full_report_20091104_en.pdf
- [2] Mou X and Chen X 2007 *Proc of MICCAI (Australia)* vol 4792 p 596
- [3] Lemacks M, Kappadath S, Shaw C, Liu X, Whitman G 2002 *Med. Phys.* **29** 1739
- [4] Kappadath S and Shaw C 2005 *Med. Phys.* **32** 3395
- [5] Kappadath S and Shaw C 2008 *Phys. Med. Biol.* **53** 5421
- [6] EUREF 2006 European guidelines for quality assurance in breast cancer screening and diagnosis 4th ed European Commission
- [7] Chung H, Ikejimba L, Kiarashi N, Samei E, Hoernig M and Lo J *Proc. SPIE 8668, Medical Imaging 2013: Physics of Medical Imaging* **86684L**
- [8] Del Medical Systems Group, Roselle, IL [Online]. Available from: <http://www.delmedical.com>.
- [9] Michail C, Spyropoulou V, Fountos G, Kalyvas N, Valais I, Kandarakis I and Panayiotakis G 2011 *IEEE Trans. Nucl. Sci.* **58** 314
- [10] Seferis I, Michail C, Valais I, Fountos G, Kalyvas N, Stromatia F, Oikonomou G, Kandarakis I, Panayiotakis G. 2013 *Nucl. Instrum. Meth. Phys. Res. A.* **729** 307
- [11] Price BD, Gibson AP, Tan LT and Royle GJ 2010 *Phys. Med. Biol.* **55** 1177
- [12] Boone JM and Chavez AE 1996 *Med. Phys.* **23**, 1997
- [13] Billas I, 2011, Angiogenesis measurements in mammography using time-resolved dual energy analysis, MSc thesis, University of Patras. Available online: <http://nemertes.lis.upatras.gr/jspui/handle/10889/4869>
- [14] Ducote JL, Xu T and Molloy S 2007 *Phys. Med. Biol.* **52** 183
- [15] ACR 1999 Mammography, Quality Control Manual (Reston, VA: Americal College of Radiology)
- [16] Boone J 1999 *Radiol.* **213** 23
- [17] Koukou V, Martini N, Michail C, Sotiropoulou P, Fountzoula C, Kalyvas N, Kandarakis I, Nikiforidis G, Fountos G. 2015 *Comput. Math. Methods Med.* [in print]